Novel Fabrication of Nanoporous Alumina Membrane Microtubes: 2-Dimensional Nanoporous Arrays on Every Facets of Microtubes

Weon-Sik Chae, Sung-Jae Im, Jin-Kyu Lee,† and Yong-Rok Kim*

Photon Applied Functional Molecule Research Laboratory, Department of Chemistry, Yonsei University, Seoul 120-749, Korea
**E-mail: yrkim@yonsei.ac.kr*
†School of Chemistry, Seoul National University, Seoul 151-742, Korea
Received December 15, 2004

Free-standing nanoporous alumina membrane microtubes with different shapes (rectangular and cylindrical tubes) and variable dimensions were easily fabricated by direct anodization of the aluminum templates of the specified shapes (strip and wire) and dimensions during the electrochemical reaction.

Key Words : Nanoporous, Anodic alumina, Microtube, Rectangular, Cylindrical

Introduction

During the last several decades, many investigations have been focused on porous anodic alumina (PAA) due to its merits of tunable nanopore diameter and long-range ordered feature of the porous nanochannels in macroscopic domain.[1,2] The pore diameter of the PAA nanochannel can precisely be controlled from a few nanometers to several hundreds of nanometers by applying pertinent electrolyte, voltage (or current), and reaction temperature during the electrochemical anodization reaction of aluminum substrate.[3] Moreover, reaction time provides a tunability in the thickness of the porous nanochannels from a hundred of nanometers to a hundred of micrometers.[1,4] Such easy control ability of the pore diameter and the thickness makes the PAA one of the interesting materials which are frequently being applied in nanoscience. So far, the studies which utilize the PAA have been performed in a wide range of research fields such as nanomaterial design,[5] molecular sieving,[6] photonic and optical device,[7] and catalysis.[8]

Recently, there have been new trials for the modification of the PAA morphology beyond the typical 2-dimensional (2D) plate membrane; the PAA membrane was micro-patterned to specific morphology with the assistance of lithographic techniques[9] and the porous alumina macrotubes were electro-chemically fabricated in millimeter scale with the partial support of tubular aluminum template.[10] Furthermore, it was also reported that a tubular porous alumina membrane coated with platinum layer provides high catalytic conversion activity for phenol production from benzene.[11] Although such promising properties are expected with the nanoporous materials of a specific morphology, the fabrication process still requires many elaborated techniques for the morphology and the dimension controls of the nanoporous materials.

In this study, a simple method is presented for the morphology and the dimension controls of the free-standing PAA membrane microtubes without the utilization of any elaborated instrumental works. This simple control of the PAA membrane microtubes is accomplished only by applying the same typical two-step anodization process[12] except for the different shapes (strip and wire) of the utilized aluminum templates from the previous simple plate-type aluminum substrate.

Experimental Section

For the shape and the dimension controls of the PAA membrane microtubes, three aluminum templates with various shapes and dimensions were utilized for the electrochemical anodization: An aluminum strip with a dimension of 250 μm × 800 μm and two aluminum wires with the diameters of 250 μm and 1 mm. An aluminum foil (99.999%, 100 mm × 100 mm) with a thickness of 250 μm and wires (99.999%) with the diameters of 1 mm and 250 μm were purchased from Aldrich. The aluminum foil was striped to a dimension of 800 μm in width before the anodization reaction.

The PAA membrane microtubes were prepared by applying the typical two-step anodizing process (Scheme 1).[12] The aluminum substrates were degreased in acetone and were electropolished in a mixed electrolyte solution of

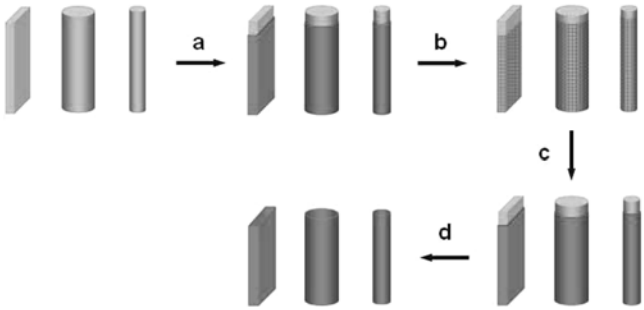

Scheme 1. Schematic drawing for the formation of 3D controlled morphologies of the PAA membrane microtubes from the aluminum templates of the corresponding specific shapes and dimensions: (a) First anodization of the aluminum templates of various shapes and dimensions, (b) etching of the initially produced alumina layer, (c) second anodization of the aluminum templates, and (d) formation of free-standing PAAs membrane microtubes by removal of the core aluminum template and the alumina barrier.

perchloric acid and ethanol (20 : 80 by volume) at a constant voltage of 14 V and 0-5 °C for 5 minutes. The aluminum substrates were then anodized galvanostatically in 2.0 wt.-% oxalic acid aqueous electrolyte solution (pH = 1.8) at a constant voltage of 40 V and 16 °C. The aluminum templates were placed in the electrolyte solution with a depth of 1-5 mm, which was located between two carbon cathodes (4 cm × 4 cm) being separated by ~4 cm. The anodic alumina layer which was generated by first anodization for 2 hours was removed by the aqueous solution of phosphoric acid (6.0 wt.-%) and chromic acid (1.8 wt.-%) at 60 °C. The second anodization was performed for 5 hours under the same condition with the first anodization. The 3D PAA microtubes were obtained by dissolving the core aluminum template with concentrated mercury (II) chloride aqueous solution and were subsequently washed with ethanol and deionized water for purification. Since the utilized chromic acid and the mercury (II) chloride are of toxic chemicals, special cautions were required during the chemical processes. In order to obtain through-pore nanochannel, the barrier layer of the free-standing PAA microtubes was removed by applying the solution of 5.0 wt.-% phosphoric acid for 30 minutes. The rectangular PAA membrane microtube appears to have the hardness enough for regular handling, however, the cylindrical membrane microtubes are somewhat brittle under a stressed pressure. Nevertheless, the cylindrical membrane microtubes also have some rigidity enough to endure a series of sample treatments and the morphology characterization.

The resulting 3D shape-controlled microtubular membranes were investigated by a microscope (Peak Stand Microscope, Japan) with a typical magnification of ×50 and a FE-SEM (JEOL, JSM-6700F). These microtubular samples were loaded onto a carbon tape, and they were subjected to the FE-SEM measurements.

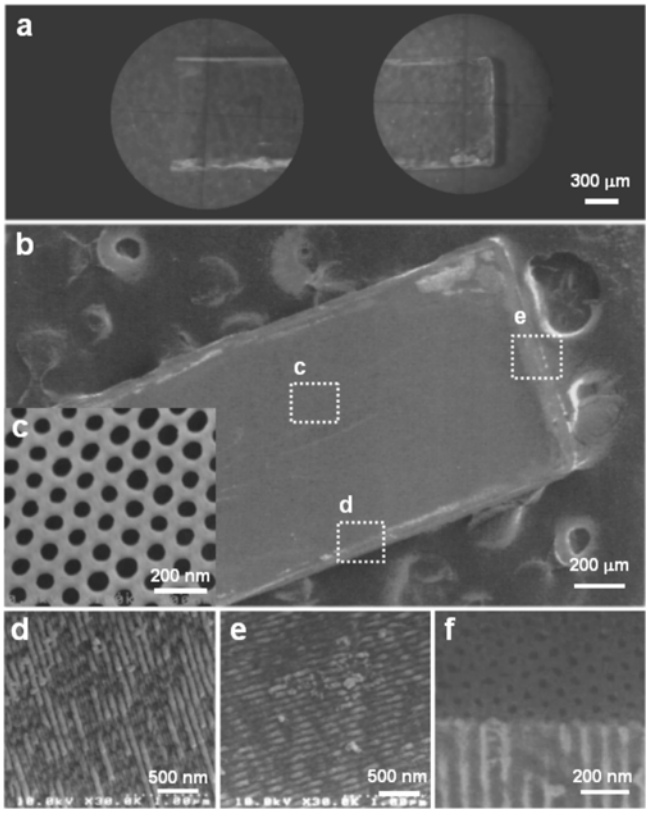

Figure 1. (a) Microscopic image of the rectangular PAA membrane microtube with a dimension of 800 μm × 250 μm in width. FE-SEM images present the detailed structural feature for the 3D rectangular microtube: (b) The low magnification and (c) high magnification images of the wide-side, (d) the narrow-side, and (e) the bottom-side. It is clearly shown that the porous nanochannels are vertically grown on every facets of the utilized aluminum strip template. (f) The inner surface image in corner part of the barrier removed rectangular PAA membrane microtube which presents through-pore nanochannels. The image was obtained with the edge part of a broken PAA membrane microtube.

Results and Discussion

As the second anodization of the aluminum template was conducted in the aqueous oxalic acid electrolyte at a constant voltage of 40 V, transparent alumina layer was formed on the surface of the utilized aluminum template of the strip shape. After removal of the core aluminum template and the alumina barrier in static condition with the concentrated mercury chloride and the phosphoric acid aqueous solutions, respectively, an interesting 3D morphology of free-standing rectangular membrane microtube could easily be obtained (Figure 1). The resulting rectangular PAA membrane microtube well resembles with the shape and dimension of the utilized strip-shaped aluminum template, and this tube is shown to be transparent in visible range (Figure 1a). Furthermore, the macroscopic height of the alumina membrane microtube could simply be varied in the range of 1-5 mm depending on the initial dipping depth of the aluminum template into the electrolyte solution. Although it was expected that each surface of the aluminum template experienced different electric field due to the geometrical difference between the aluminum template and the electrodes, the alumina layer was formed on the 3-dimentional every surfaces with the similar thickness. From the observed result, it is considered that the PAA layer growing is not very sensitive in the experimental condition of ours.

Field-emission scanning electron microscope (FE-SEM) images show the detailed structural feature of the outer surface for the rectangular membrane microtube. It is shown that the PAA layer with a thickness of ~40 μm is grown on the surface of the aluminum strip in all directions and presents the well-ordered porous nanochannel array; the porous nanochannel grows outward on both the side surfaces (Figure 1c and d) and grows downward on the bottom surface of the aluminum strip template (Figure 1e). The magnified image of the rectangular PAA membrane microtube shows the unique well-defined porous nanochannel array with an average pore diameter of 60 nm and a pore density of ~1×10^{10}/cm^2 in all directions.

Anodization of the aluminum wire with a diameter of 1 mm also produced the transparent anodic alumina layer on

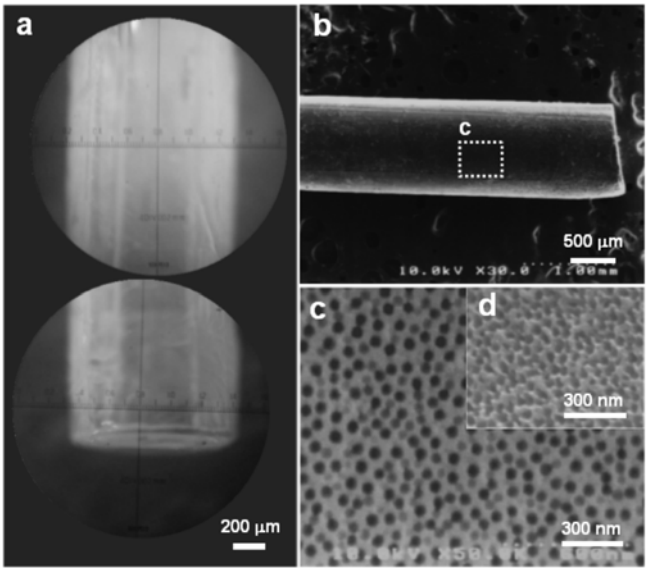

Figure 2. (a) Microscopic image of the cylindrical PAA membrane microtube with a dimension of ~1 mm in diameter. FE-SEM images present the detailed structural feature for the cylindrical microtube: (b) The low and (c) high magnification images of the side surface. The porous nanochannels are vertically grown on every surfaces of the aluminum wire template. (d) The inner surface image of the barrier removed cylindrical PAA membrane microtube which presents through-pore nanochannels.

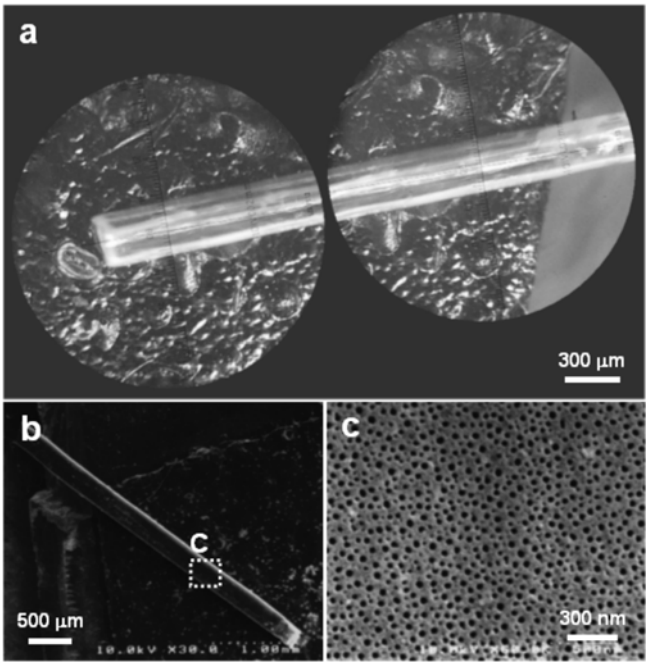

Figure 3. (a) Microscopic image of the cylindrical PAA membrane microtube with a dimension of ~250 μm in diameter. FE-SEM images present the detailed structural feature for the cylindrical PAA microtube: (b) The low and (c) high magnification images on the side surface. The magnified image of the outer surface of the cylindrical membrane microtube shows the unique nanopores with an average diameter of 50 nm.

its surface. A free-standing cylindrical PAA membrane microtube with a membrane thickness of ~40 μm can be conveniently obtained after removal of the core aluminum wire template and the alumina barrier (Figure 2). FE-SEM image for the PAA membrane microtube presents the unique 3D morphology of the cylindrical shape (Figure 2b), and the magnified image of the outer and inner surfaces of the cylindrical membrane microtube shows the unique through-pore nanochannels with the pore diameter of 50-60 nm as shown in Figure 2c and d. Moreover, as the smaller aluminum wire template (250 μm in diameter) was utilized for the anodization, the smaller cylindrical membrane microtube could also be obtained (Figure 3). All the resulting cylindrical PAA membrane microtubes are shown to be optically transparent in visible range.

These 3D shape-controlled PAA membrane microtubes with variable dimensions have the high potential for the applications as catalytic and/or photocatalytic membrane reactors which have an additional function of biomolecular sieving. Conventional alumina membrane reactors with tubular morphology have the limitation in the fine size-control of the nanopores.[13] However, our free-standing PAA nanoporous membrane microtubes have the great advantage of the easy tunabilities of the nanopore diameter and the morphology including the dimension.

In summary, the simple fabrication of the 3D shape-controlled nanoporous membrane microtubes (rectangular and cylindrical shapes) with various dimensions is presented by direct utilization of the aluminum templates of the specified morphology and dimension. The resulting PAA membrane microtubes well preserve, in 3D domains, the unique 2D array of the porous nanochannels on its every facets with the well-defined pore diameter. Therefore, this simple fabrication method of free-standing nanoporous membrane microtube will hopefully provide a new opportunity for the development of noble porous materials in the application fields of nano- and bio-molecular systems and catalysis.

Acknowledgement. This work is financially supported by a grant from National Research Laboratory (NRL) (grant No. M1-0302-00-0027) program administered by MOST.

References

1. Diggle, J. W.; Downie, T. C.; Goulding, C. W. *Chem. Rev.* **1969**, *69*, 365.
2. Li, F.; Zhang, L.; Metzger, R. M. *Chem. Mater.* **1998**, *10*, 2470.
3. (a) Martin, C. R. *Science* **1994**, *266*, 1961. (b) Li, A. P.; Müller, F.; Birner, A.; Nielsch, K.; Gösele, U. *J. Appl. Phys.* **1998**, *84*, 6023. (c) Lee, W.; Lee, J.-K. *Adv. Mater.* **2002**, *14*, 1187.
4. (a) Ohij, N.; Enomoto, N.; Mizushima, T.; Kakuta, N.; Morioka, Y.; Ueno, A. *J. Chem. Soc., Faraday Trans.* **1994**, *90*, 1279. (b) Asoh, H.; Nishio, K.; Nakao, M.; Tamamura, T.; Masuda, H. *J. Electrochem. Soc.* **2001**, *148*, B152. (c) Gasparac, R.; Kohli, P.; Mota, M. O.; Trofin, L.; Martin, C. R. *Nano Lett.* **2004**, *4*, 513.
5. (a) Martin, B. R.; Dermody, D. J.; Reiss, B. D.; Fang, M.; Lyon, L. A.; Natan, M. J.; Mallouk, T. E. *Adv. Mater.* **1999**, *11*, 1021. (b) Routkevitch, D.; Bigioni, T.; Moskovits, M.; Xu, J. M. *J. Phys. Chem.* **1996**, *100*, 14037. (c) Lahav, M.; Sehayek, T.; Vaskevich, A.; Rubinstein, I. *Angew. Chem., Int. Ed.* **2003**, *42*, 5576. (d) Suh, J. S.; Lee, J. S. *Appl. Phys. Lett.* **1999**, *75*, 2047. (e) Lee, W.; Yoo,

H.-I.; Lee, J.-K. *Chem. Commun.* **2001**, 2530. (f) Lee, J.-K.; Koh, W.-K.; Chae, W.-S.; Kim, Y.-R. *Chem. Commun.* **2002**, 138. (g) Steinhart, M.; Wendorff, J. H.; Greiner, A.; Wehrspohn, R. B.; Nielsch, K.; Schilling, J.; Choi, J.; Gösele, U. *Science* **2002**, *296*, 1997. (h) Lee, J. S.; Suh, J. S. *Bull. Korean Chem. Soc.* **2003**, *24*, 1827.

6. (a) Lee, S. B.; Mitchell, D. T.; Trofin, L.; Nevanen, T. K.; Söderlund, H.; Martin, C. R. *Science* **2002**, *296*, 2198. (b) Yamaguchi, A.; Uejo, F.; Yoda, T.; Uchida, T.; Tanamura, Y.; Yamashita, T.; Teramae, N. *Nature Mater.* **2004**, *3*, 337.
7. (a) Mikulskas, I.; Juodkazis, S.; Toǹasiunas, R.; Dumas, J. G. *Adv. Mater.* **2001**, *13*, 1574. (b) Govyadinov, A.; Emeliantchik, I.; Kurilin, A. *Nucl. Inst. Met. Phys. Res. A* **1998**, *419*, 667. (c) Delendik, K.; Emeliantchik, I.; Litomin, A.; Rumyantsev, V.; Voitik, O. *Nucl. Phys. B* **2003**, *125*, 394. (d) Kukhta, A. V.; Gorokh, G. G.; Kolesnik, E. E.; Mitkovets, A. I.; Taoubi, M. I.; Koshin, Y. A.; Mozalev, A. M. *Surf. Sci.* **2002**, *507-510*, 593.
8. (a) Patermarakis, G.; Pavlidou, C. *J. Catal.* **1994**, *147*, 140. (b) Patermarakis, G.; Nicolopoulos, N. *J. Catal.* **1999**, *187*, 311.
9. (a) Li, A.-P.; Müller, F.; Birner, A.; Nielsch, K.; Gösele, U. *Adv. Mater.* **1999**, *11*, 483. (b) Yan, J.; Rama Rao, G. V.; Barela, M.; Brevnov, D. A.; Jiang, Y.; Xu, H.; López, G. P.; Atanassov, P. B. *Adv. Mater.* **2003**, *15*, 2015.
10. (a) Gong, D.; Yadavalli, V.; Paulose, M.; Pishko, M.; Grimes, C. A. *Biomed. Microdev.* **2003**, *5*, 75. (b) Mizushima, T.; Matsumoto, K.; Sugoh, J.; Ohkita, H.; Kakuta, N. *Appl. Catal., A: Gen.* **2004**, *265*, 53.
11. Niwa, S.; Eswaramoorthy, M.; Nair, J.; Raj, A.; Itoh, N.; Shoji, H.; Namba, T.; Mizukami, F. *Science* **2002**, *295*, 105.
12. Masuda, H.; Satoh, M. *Jpn. J. Appl. Phys.* **1996**, *35*, L126.
13. Coronas, J.; Santamaría, J. *Catal. Today* **1999**, *51*, 377.